LAMINAR FLOW WITH INJECTION IN A STRAIGHT DUCT

A. A. Repin

UDC 532.517.2

The velocity distribution and pressure drop associated with injection flow in a straight duct are analyzed on the basis of exact solutions of the Navier–Stokes equations.

The analytical investigation of flows with transverse injection is normally carried out on the assumption that the flow near the wall has boundary-layer properties (see, e.g. [1, 2]), corresponding to small injection rates. For large injection rates, such that transverse pressure gradients are set up and the transverse flow velocities v are comparable with the longitudinal flow velocities u, the flow pattern can no longer be described in terms of a simple model. In particular, for values of the injection parameter above the critical value, boundary-layer separation takes place, and near the wall, as clearly shown by, for example, the results of visual observations [3], there emerges a flow region that can be analyzed only on the basis of the complete system of Navier–Stokes equations.

If, however, injection is realized into a duct ($0 < x < \infty$) of finite height ($0 < y < h$), at a certain distance $x = x^*$ from the channel entry the boundary layer displaced by injection at $y = 0$ joins with the boundary layer at $y = h$, and the transverse velocity profile stabilizes. The principal attribute of this kind of flow in the laminar regime is self-similarity; accordingly, for $x \geq x_0 > x^*$ the solution can be written

$$u = u_0(y) - (x - x_0)\dot{\Phi}(y),\ v = \Phi(y),\ p = p_0(y) + (x - x_0)p_1 + (x - x_0)^2 p_2. \quad (1)$$

Inserting (1) into the Navier–Stokes equations, we obtain a system of ordinary differential equations:

$$\nu\dddot{\Phi} = -\frac{2p_2}{\rho} + \Phi\ddot{\Phi} - \dot{\Phi}^2, \quad (2)$$

$$\nu\ddot{u}_0 = \frac{p_1}{\rho} + \dot{u}_0\Phi - u_0\dot{\Phi}, \quad (3)$$

$$\frac{p_0}{\rho} = \text{const} + \nu\dot{\Phi} - \frac{1}{2}\Phi^2, \quad (4)$$

in which the dot denotes differentiation with respect to y. Here the longitudinal velocity $u_0(y)$ corresponds to the flow entering the channel up to a cross section $x = x_0 > x^*$ with a specified volumetric flow rate $Q_0 = \int_0^h u_0 dy = \bar{u}h$. The variation of the flow rate along the channel due to injection at $x \geq x_0$ is related to the quantity $\dot{\Phi}$ and the total flow rate:

$$Q = \int_0^h [u_0(y) - (x - x_0)\dot{\Phi}(y)]\, dy = Q_0 - (x - x_0)(v_1 - v_0), \quad (5)$$

where v_0 and v_1 are the transverse velocities at the respective boundaries $y = 0$ and $y = h$.

The quantities p_1 and p_2 are constants. Here p_1 is determined in the solution of Eq. (3) for $u_0(y)$ subject to the boundary conditions $u_0(0) = u_0(h) = 0$ and a given flow rate Q_0, and p_2 is determined in the solution of the third-order equation (2) under four boundary conditions:

$$\Phi(0) = v_0,\ \Phi(h) = v_1,\ \dot{\Phi}(0) = \dot{\Phi}(h) = 0. \quad (6)$$

Translated from Inzhenerno-Fizicheskii Zhurnal, Vol. 28, No. 2, pp. 272-281, February, 1975. Original article submitted May 25, 1974.

Equation (3) is completely autonomous and admits the solution $u_0 \equiv 0$. In this case the system (2)-(4) yields the velocity distribution for viscous flow in the case of injection into a duct closed at x = 0, i.e., $Q_0 = 0$ for $x_0 = 0$. In the general case of $u_0 \neq 0$ the solution of Eqs. (2) and (3) describes the pattern resulting from the addition of longitudinal and transverse viscous fluid flows, thus affording a "viscous" generalization of the superposition principle for flows of an ideal fluid.

We also note that the given flow generalizes in a certain sense flows of the boundary-layer type by eliminating the influence of the transverse pressure gradient p_0 (through $\dot{\Phi}$ and Φ^2) on the transverse distribution of the longitudinal velocities in plane-parallel flow.

In accordance with (1) the distribution of the temperature T (or concentration C) is also self-similar:

$$T = \vartheta_0(y) + (x - x_0)\vartheta(y), \tag{7}$$

where $\vartheta_0(y)$ and $\vartheta(y)$, according to the heat-transfer equation, satisfy the differential equations

$$a\ddot{\vartheta}_0 = \Phi\dot{\vartheta}_0 + u_0\vartheta, \tag{8}$$

$$a\ddot{\vartheta} = \Phi\dot{\vartheta} - \dot{\Phi}\vartheta, \tag{9}$$

in which a is the thermal diffusivity.

The indicated self-similarity is not the exclusive property of planar motion. An analogous solution exists for axisymmetrical motion as well:

$$\begin{gathered} u = u_0(r) + (x - x_0)\pi(r), \quad v = \varphi(r), \quad w = \chi(r), \\ p = p_0(r) + (x - x_0)p_1 + (x - x_0)^2 p_2 \quad (r_1 < r < r_2, \; 0 < x < \infty), \end{gathered} \tag{10}$$

where v, w, and u are, respectively, the radial, circumferential, and longitudinal components of the velocity,

$$\nu\left(\ddot{\pi} + \frac{\dot{\pi}}{r}\right) = -\frac{2p_2}{\rho} - (\pi^2 + \varphi\dot{\pi}), \tag{11}$$

$$\pi = -\frac{1}{r}(r\varphi)^{\cdot}, \tag{12}$$

$$\nu\left(\ddot{u}_0 + \frac{\dot{u}_0}{r}\right) = \frac{p_1}{\rho} + u_0\pi + \dot{u}_0\varphi, \tag{13}$$

$$\dot{p}_0 = \nu\left(\ddot{\varphi} + \frac{\dot{\varphi}}{r} - \frac{\varphi}{r^2}\right) - \varphi\dot{\varphi} - \frac{\chi^2}{r}, \tag{14}$$

$$\nu\left(\ddot{\chi} + \frac{\dot{\chi}}{r} - \frac{\chi}{r^2}\right) = \varphi\dot{\chi} + \frac{\varphi\chi}{r}, \tag{15}$$

and the dot denotes differentiation with respect to r.

Equations (11)-(15) can be used to analyze the flow generated by injection into an annular duct. It is to be noted that this self-similarity also holds for nonsteady flows. Omitting the exact corresponding system of equations, we point out that time derivatives are added to the left-hand sides of Eqs. (2)-(4) in the planar case: $-(\partial^2\Phi/\partial y\partial t)$ in (2), $-(\partial u_0/\partial t)$ in (3), and $\partial\Phi/\partial t$ in (4). Analogously, for the axisymmetrical case the left-hand sides of Eqs. (11)-(15) are augmented with the derivatives $-(\partial\pi/\partial t)$, $-(\partial u_0/\partial t)$, $\partial\varphi/\partial t$, $-(\partial\chi/\partial t)$.

Besides their direct applicability to the given injection problem, the indicated equations are of independent interest insofar as they supplement the restricted class of self-similar problems associated with the Navier–Stokes equations and take inertial terms into account. Their solution shows how viscous flow goes over to inviscid flow with variation of the Reynolds number Re.

We give the results of the calculations for the steady planar flow equations (2)-(4).

1. The transverse velocity equation (2) is similar in its structure to the Falkner–Skan equations and boundary-layer theory. However, because the boundary conditions differ, the similarity vanishes in the solutions. In the general case Eq. (2) does not submit to elementary integration.

On the other hand, if the injection (suction) rate at y = 0 is equal to the suction (injection) rate at

$y = h$, i.e., if $v_1 = v_0$, then v = const and $p_2 = 0$. This situation is characterized by the absence of a transverse pressure gradient (p_0 = const). Inasmuch as this result does not depend on u_0, it can be assumed that the transverse flow does not induce an additional pressure gradient in the longitudinal flow. Its inception requires that $v_1 \neq v_0$.

Let it be supposed that the duct wall $y = h$ is impermeable, i.e., that $v_1 = 0$. Clearly, the two-sided injection problem ($v = v_0$ at $y = 0$ and $v_1 = -v_0$ at $y = h$) is also reducible to the foregoing case, because on the duct axis $\Phi(h/2) = \dot{\Phi}(h/2) = 0$.

Equation (2) subject to the boundary conditions (6)

$$\Phi(0) = v_0,\ \dot{\Phi}(0) = \Phi(h) = \dot{\Phi}(h) = 0 \tag{1.1}$$

has been solved numerically. For implementation of the numerical procedure it is written in the integral form

$$\begin{gathered}\Phi = \Phi_0(y) + \int_0^1 K_1(y,\ \eta)\,\Phi(\eta)\,d\eta + \int_0^1 K_2(y,\ \eta)\,\Phi^2(\eta)\,d\eta + \int_0^1 K_3(y,\ \eta)\,\dot{\Phi}^2(\eta)\,d\eta,\\ \beta \equiv \frac{2p_2h^2}{\rho v_0^2} = a_0(\mathrm{Re}) + \int_0^1 k_1(\eta)\,\Phi(\eta)\,d\eta + \int_0^1 k_2(\eta)\,\Phi^2(\eta)\,d\eta + \int_0^1 k_3(\eta)\,\dot{\Phi}^2(\eta)\,d\eta,\end{gathered} \tag{1.2}$$

which is obtained as follows. We denote by Φ^* and Φ^{**} certain average values of Φ and $\dot{\Phi}$ over the duct height and write Eq. (2) in the form

$$\nu\dddot{\Phi} - \Phi^*\ddot{\Phi} + \Phi^{**}\dot{\Phi} = H, \tag{1.3}$$

where

$$H = -\frac{2p_2}{\rho} + (\Phi - \Phi^*)\ddot{\Phi} - (\dot{\Phi} - \Phi^{**})\,\dot{\Phi}. \tag{1.4}$$

The formal integral (1.3) has the form

$$\Phi = D + C_1 \exp\left(\mu_1 \frac{y}{h}\right) + C_2 \exp\left(\mu_2 \frac{y}{h}\right) + \int_0^y K(y-\eta)\,H(\eta)\,(y-\eta)\,d\eta, \tag{1.5}$$

where

$$\mu_{1,2} = \frac{\Phi^*}{v_0}\frac{\mathrm{Re}}{2} \pm \sqrt{\left(\frac{\Phi^*}{v_0}\right)^2 \frac{\mathrm{Re}^2}{4} - \frac{\Phi^{**}h}{v_0}\mathrm{Re}},\quad \mathrm{Re} = \frac{v_0 h}{\nu}, \tag{1.6}$$

$$K(y-\eta) = \frac{C}{\mu_1 - \mu_2}\left[\exp\left(\mu_1 \frac{y-\eta}{h}\right) - \exp\left(\mu_2 \frac{y-\eta}{h}\right)\right]. \tag{1.7}$$

Transforming (1.5) with regard for the boundary conditions (1.1) governing C_1, C_2, D, and $2p_2/\rho$, we arrive at (1.2). Without writing out the cumbersome expressions for the kernels K_1, K_2, K_3 in general form, we point out that the convergence of the approximations according to (1.2) depends essentially on the character of the kernels, i.e., in the final analysis on the choice of values for Φ^* and Φ^{**}. In particular, for $\Phi^* = \Phi^{**} = 0$ the approximation procedure according to Eq. (1.2) converges sufficiently rapidly for small Re; for $|\mathrm{Re}| < 1$ (regardless of the sign of Re) one approximation is adequate.

For large values of Re it is required to have $\Phi^* \neq 0$ and $\Phi^{**} \neq 0$ in order to ensure rapid convergence. The zeroth approximation in this case is given by the expression

$$\Phi_0 = v_0\left[d_0 + \beta\frac{y}{h} + d_1 \exp\left(\mu_1 \frac{y}{h}\right) + d_2 \exp\left(\mu_2 \frac{y}{h}\right)\right], \tag{1.8}$$

in which

$$\begin{gathered}\beta \equiv \frac{2p_2h^2}{\rho v_0^2} = \frac{\mu_1\mu_2(\exp\mu_1 - \exp\mu_2)}{D_0},\quad d_0 = -\beta - d_1\exp\mu_1 - d_2\exp\mu_2,\\ d_1 = -\frac{\mu_2}{D_0}[1 - \exp\mu_2],\quad d_2 = \frac{\mu_1}{D_0}[1 - \exp\mu_1],\\ D_0 = \mu_1 - \mu_2 + (\mu_1 - \mu_2)\exp(\mu_1 + \mu_2) + (\mu_1\mu_2 - \mu_1 + \mu_2)\exp\mu_2\\ - (\mu_1\mu_2 + \mu_1 - \mu_2)\exp\mu_1.\end{gathered} \tag{1.9}$$

TABLE 1. Drag and Heat-Transfer Coefficients for Laminar Injection Flow in a Straight Duct

Re, Pe	50	40	30	20	10	5	1	0,5
α(Re)	2,08	2,10	2,14	2,22	2,5	3,26	12,2	25
β(Re)	—2,62	—2,85	—3,05	—3,3	—3,8	—5,2	—14,3	—26,3
γ(Re)	—2,62	—2,85	—3,05	—3,3	—3,8	—5,1	—14,1	—26,1
Nu(Pe)	7,1	6,3	5,5	4,5	3,19	2,2	1,24	1,07
Re, Pe	—0,5	—1	—5	—10	—20	—30	—40	—50
α(Re)	—25	12,5	3,26	2,5	2,22	2,14	2,10	2,08
β(Re)	21,7	10,7	1,50	0,59	0,48	0,48	0,48	0,48
γ(Re)	21,9	10,9	1,52	0,59	0,48	0,48	0,48	0,48
Nu(Pe)	0,93	0,76	0,191	0,015	0	0	0	0

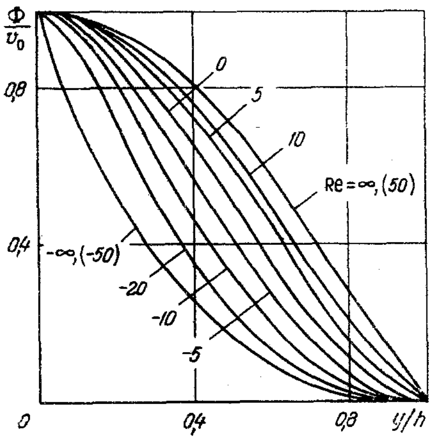

Fig. 1. Transverse velocity distribution Φ/v_0 over the height of a duct with an impermeable wall y = h ($v_1 = 0$).

Calculations show that two or three approximations suffice with practically 1% error for $\Phi^* = v_0/2$, $\Phi^{**} = -v_0/h$, and all values of Re. This is because the sign of each of the functions Φ and $\dot{\Phi}$ is constant in the interval $0 < y < h$ and so the zeroth approximation (1.8) itself, obtained by the replacement of Φ and $\dot{\Phi}$ with constants, represents the flow faithfully in every detail.

For equations of the type (2) the adopted integral method has major advantages from the convergence standpoint over the conventional difference method, because the latter requires careful selection of the duct height step for each value of Re to ensure stability (i.e., the same difficulty is met as in the solution of the complete system of Navier–Stokes equations.)

The results of a calculation of the transverse velocities over the duct height on the basis of Eq. (1.2) are given in Fig. 1 for a variation of Re from $-\infty$ (suction) to $+\infty$ (injection). It is seen that the Φ profile becomes progressively more humped with increasing Re, approaching in the limit (essentially at Re = 30) the profile for an ideal fluid. The latter is obtained by the direct solution of Eq. (2) for $\nu = 0$ with the boundary conditions $\Phi(0) = v_0$, $\dot{\Phi}(0) = \ddot{\Phi}(h) = 0$:

$$\Phi = v_0 \cos\left(\frac{\Pi}{2}\frac{y}{h}\right),\ \beta = -\frac{\Pi^2}{4},\ \dot{\Phi} = \frac{\Pi}{2}\frac{v_0}{h}\sin\left(\frac{\Pi}{2}\frac{y}{h}\right), \tag{1.10}$$

i.e., with injection, beginning with Re = 30, the transverse velocity distribution can be calculated from the ideal-fluid model. The influence of viscosity, on the other hand, which is needed in order to calculate the friction losses, only has to be taken into account in the immediate proximity of the wall y = h in a layer of thickness δ. Additional investigation shows that the thickness of this layer is of order $\delta = h(\ln \mathrm{Re}/\mathrm{Re})$.

For Re < 0 (suction at y = 0) the behavior of Φ/v_0 differs somewhat. The roundness of the profile is observed to decrease monotonically with increasing |Re|. For $|\mathrm{Re}| \geq 50$ the profile practically coincides with the asymptotic profile ($|\mathrm{Re}| = \infty$). Significantly, the latter differs from the ideal-fluid profile (1.10), which does not depend on the sign of v_0. This result confirms the well-known disparity between the vanishing-viscosity theory and the ideal-fluid theory [4].

The Φ/v_0 distribution in Fig. 1 corresponds to a longitudinal flow $u = -\dot{\Phi}x$, in whose motion the pressure drops along the duct in accordance with the expression (1.2) for p_2:

$$\Delta p_1 = p(L) - p(0) = p_2 L^2 = \frac{\rho v_0^2}{2}\left(\frac{L}{h}\right)^2 \beta(\mathrm{Re}). \tag{1.11}$$

The results of a calculation of $\beta(\mathrm{Re})$ are given in the second column of Table 1. For Re > 0 the values of $\beta(\mathrm{Re}) < 0$, where $\beta \to -2.6$ as $\mathrm{Re} \to \infty$; for values of Re close to zero $\beta = -(12/\mathrm{Re} + 81/35)$; for Re < 0 the values of $\beta(\mathrm{Re}) > 0$, and $\beta \to 0.48$ as $|\mathrm{Re}| \to \infty$.

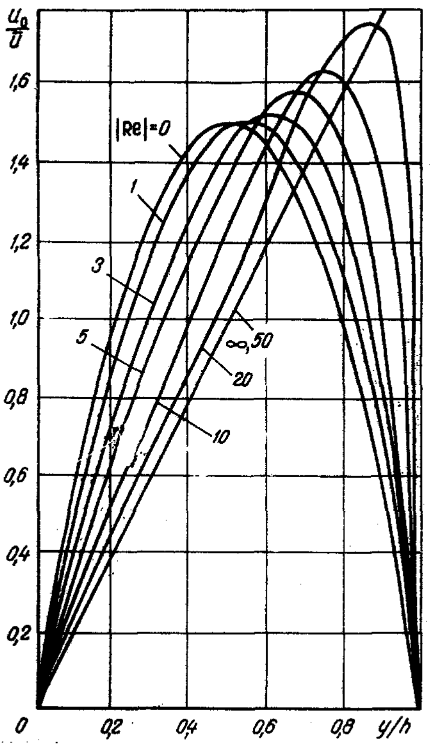

Fig. 2. Longitudinal velocity distribution u_0 over the duct height for $v_1 = v_0$.

2. Next we consider the longitudinal velocity distribution, which, as implied by (1), consists of two components. Equations (3) enable us to determine the component $u_0(y)$ corresponding to the initial cross section $x = x_0$ and the flow rate Q_0 specified in that cross section. The rate Q_0 is clearly equal to the sum of the flow rate entering the duct through the entrant cross section $x = 0$ and the flow rate $(v_1 - v_0)x_0$ due to injection in the initial section of the duct $(0 < x < x_0)$. Inasmuch as the cross section $x = x_0 > x^*$ is arbitrary (by the statement of the problem) and any other cross section $x > x_0$ can be taken as the initial, we can express the longitudinal velocity distribution in any cross section $x > x_0$ in terms of $u_0(y)$, i.e., $u(x, y) = c(x)u_0(y)$. We show that this is indeed the case. In correspondence with (5) we have

$$c(x) = \int_0^h u(x, y)\,dy \Big/ \int_0^h u_0(y)\,dy = 1 - \frac{(x - x_0)(v_1 - v_0)}{Q_0}$$

and in correspondence with (1)

$$u_0(y) - (x - x_0)\,\Phi(y) = u_0(y)\left[1 - \frac{(x - x_0)(v_1 - v_0)}{Q_0}\right].$$

It follows from the latter relation that

$$u_0(y) = \frac{Q_0}{v_1 - v_0}\,\Phi. \tag{2.1}$$

Substituting (2.1) into (3), we see at once that $\dot{\Phi}$ does satisfy (2) for

$$2p_2 = -p_1\frac{v_1 - v_0}{Q_0}, \tag{2.2}$$

and so, in fact, $u(x, y) = c(x)u_0(y)$.

Thus, to obtain the longitudinal velocity profile in any cross section it suffices to solve Eq. (3) for the selected cross section $x = x_0$.

For $v = \text{const}$ $(v_1 = v_0)$ and the boundary conditions $u_0(0) = u_0(h) = 0$ Eq. (3) has the solution

$$u_0 = \frac{p_1 h}{\rho v_0}\left[\frac{\exp\left(\mathrm{Re}\,\frac{y}{h}\right) - 1}{\exp \mathrm{Re} - 1} - \frac{y}{h}\right], \quad \mathrm{Re} = \frac{v_0 h}{\nu}. \tag{2.3}$$

The constant p_1 is expressed in terms of the given flow rate $Q_0 = \bar{u}h$:

$$\frac{p_1}{\rho} = -\frac{\bar{u}v_0}{h}\,\alpha(\mathrm{Re}), \quad \alpha(\mathrm{Re}) = \left[\frac{1}{2} - \frac{1}{\mathrm{Re}} + \frac{1}{\exp \mathrm{Re} - 1}\right]^{-1}, \tag{2.4}$$

and the values of $\alpha(\mathrm{Re})$ are given in the first column of Table 1. The pressure drop along the duct is

$$\Delta p_{\parallel} = p_1 L = -\rho\bar{u}v_0\frac{L}{h}\,\alpha(\mathrm{Re}). \tag{2.5}$$

The flow regime without a transverse component (Poiseuille flow) corresponds to $\mathrm{Re} = 0$, $\alpha \to 12/\mathrm{Re}$, and by passage to the limit we obtain the well-known result $\Delta p = -12\nu\rho\bar{u}(L/h)$; as $|\mathrm{Re}| \to \infty$ (essentially $|\mathrm{Re}| \geq 50$) $|\alpha| = 2$, i.e., for $|\mathrm{Re}| \gg 1$ the drag increases appreciably:

$$\Delta p_{\parallel} = -2\rho\,|v_0|\,\bar{u}\,\frac{L}{h}. \tag{2.6}$$

The considerable increase in Δp is attributable to a change in the structure of the velocity profile, which is drawn closer to the wall $y = h$ (to $y = 0$ for $\mathrm{Re} < 0$) (Fig. 2), causing the velocity gradient u_0 to increase significantly there; for $|\mathrm{Re}| \gg 1$ the velocity increases linearly along the height of the duct, dropping to zero only in the immediate vicinity of $y = h$. Equation (3) has been solved numerically for $v_1 = 0$, as in the case of (2) by the integral method. In principle, since u_0 is expressed in terms of $\dot{\Phi}$ according to (2.1),

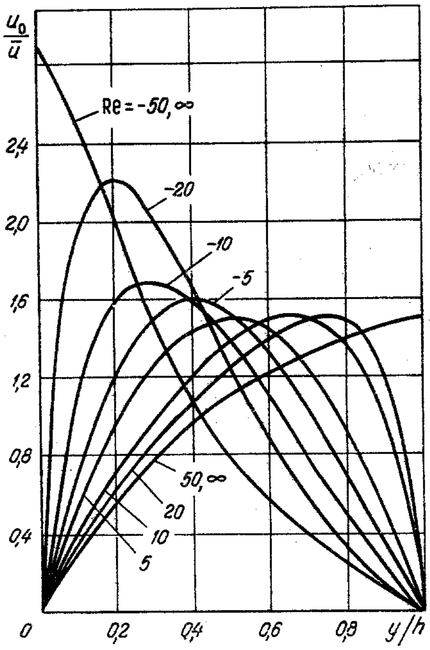

Fig. 3. Longitudinal velocity distribution u_0 over the height of a duct with an impermeable wall $y = h$ ($v_1 = 0$).

we can use the results of the numerical integration for Φ in §1. However, to avoid the inevitable errors of numerical differentiation, we form an integral equation for the determination of u_0. Accordingly, we write (3) in the form

$$\nu\ddot{u}_0 - \dot{u}_0\Phi^* + u_0\Phi^{**} = p_1 + G. \tag{2.7}$$

The formal integration of (2.7) with regard for the boundary conditions $u_0(0) = u_0(h) = 0$ yields the integral equation

$$u_0 = u_{00} + \mathrm{Re}\int_0^1 K(y,\ \eta)\, u_0 d\eta, \quad \gamma \equiv \frac{p_1 h}{\rho v_0 \bar{u}} = b_0(\mathrm{Re}) + \int_0^1 \frac{u_0}{\bar{u}} k(\eta)\, d\eta, \tag{2.8}$$

in which u_{00} satisfies Eq. (2.7) for $G = 0$ and has the form

$$u_{00} = \bar{u}\gamma_0(\mathrm{Re})\left[\frac{(1-\exp\mu_2)\exp\left(\mu_1\frac{y}{h}\right) + (\exp\mu_1 - 1)\exp\left(\mu_2\frac{y}{h}\right)}{\exp\mu_1 - \exp\mu_2} - 1\right], \tag{2.9}$$

$$\gamma_0(\mathrm{Re}) = \left[\frac{(1-\exp\mu_2)(\exp\mu_1 - 1)}{\exp\mu_1 - \exp\mu_2}\,\frac{\mu_2 - \mu_1}{\mu_1\mu_1} - 1\right]^{-1}, \tag{2.10}$$

where μ_1 and μ_2 are evaluated according to Eq. (1.6).

The calculations for $\Phi^* = v_0/2$ and $\Phi^{**} = -v_0/h$ exhibit a weak influence of the Φ profile on the distribution of u_0; the difference in the values obtained for the Φ profiles (1.2), (1.8), and (1.10) does not exceed 5%. Also weak is the influence on the quantity

$$\Delta p_{\parallel} = p_1 L = \rho v_0 \bar{u}\frac{L}{h}\gamma(\mathrm{Re}), \tag{2.11}$$

where p_1 is evaluated in terms of $\gamma(\mathrm{Re})$ according to (2.8).

The velocity profiles u_0 given in Fig. 3 indicate that the asymptotic representations for $|\mathrm{Re}| = \infty$ can be used for $|\mathrm{Re}| \geq 50$; as in the case of Φ, there is a disparity between the asymptotic representations for $\mathrm{Re} = +\infty$ and $\mathrm{Re} = -\infty$. The values of $\gamma(\mathrm{Re})$ are given in Table 1. We note that the values of γ and β practically coincide, as expected in light of the above-indicated exact relation (2.2). This result clearly shows the acceptable accuracy of computational procedures based on the integral relations (1.2) and (2.8). The asymptotic values of γ and β are: $\gamma(\mathrm{Re} > 50) = \beta(\mathrm{Re} > 50) = -2.62$; $\gamma(\mathrm{Re} < -50) = \beta(\mathrm{Re} < -50) = 0.48$; for small $|\mathrm{Re}| < 0.5$ we have $\gamma = \beta = -12(1/\mathrm{Re} + 3/35)$.

According to (1), taking Eqs. (1.11) and (2.11), as well as the equality of γ and β, into account, we write the total pressure drop in the form

$$\Delta p = \Delta p_{\perp} + \Delta p_{\parallel} = \gamma(\mathrm{Re})\left[\frac{\rho v_0^2}{2}\left(\frac{L}{h}\right)^2 + \rho v_0 \bar{u}\frac{L}{h}\right]. \tag{2.12}$$

3. We now apply the results obtained above to the following heat problem: We consider two parallel surfaces $y = 0$ and $y = h$, the first at a temperature T_0 and the second at a temperature T_w. To characterize the heat-transfer rate between the surfaces we introduce the number $\mathrm{Nu} = \alpha h/\lambda = [1/(T_w - T_0)](\partial T/\partial y)|_{y=h}$, where the heat-transfer coefficient α is referred to the temperature difference $T_w - T_0$. It is obvious that in this stabilized thermal regime without injection the mutual influence between the walls is through heat conduction, and $\mathrm{Nu} = 1$. Suppose now that injection (suction) is realized at $y = 0$ with a temperature T_0. Expressions (6) and (7) imply that $\vartheta = 0$ due to the invariance of T_0 and T_w along x.

The solution of Eq. (8) for ϑ_0 with $u_0 = 0$ yields the expression

$$\vartheta_0 = T_0 + (T_w - T_0)\int_0^y \exp\left[\mathrm{Pe}\int_0^y \varphi dy\right] dy\left[\int_0^1 \exp\left(\mathrm{Pe}\int_0^y \varphi dy\right) dy\right]^{-1}, \quad \mathrm{Pe} = \mathrm{Pr}\,\mathrm{Re}, \tag{3.1}$$

which corresponds to

$$\mathrm{Nu} = \exp\left(\mathrm{Pe}\int_0^1 \varphi dy\right)\left[\int_0^1 \exp\left(\mathrm{Pe}\int_0^y \varphi dy\right) dy\right]^{-1}. \tag{3.2}$$

The dependence Nu(Pe) for φ determined by the solution of Eq. (1.2) with $v_1 = 0$ and $v_0 \neq 0$ is given in the fourth column of Table 1. It is seen that the injection rate has a strong influence on the heat transfer; $Nu \sim \sqrt{Pe}$ for $Pe \gg 1$. In the suction case ($Pe < 0$) the influence of the surface $y = 0$ on the surface $y = h$ diminishes, vanishing altogether for $Pe \approx -20$.

If in this case the surface $y = h$ is permeable ($v_1 = v_0$, $\varphi = \text{const}$), we obtain a simple expression from (3.2):

$$Nu = \frac{Pe \exp Pe}{\exp Pe - 1}. \tag{3.3}$$

Qualitatively the same results are obtained, but quantitatively they are more accentuated; $Nu \sim Pe$ for $Pe \gg 1$, and in suction ($Pe < 0$) the influence of the surface $y = 0$ on the surface $y = h$ essentially vanishes for $Pe \leq -5$.

NOTATION

x, y	are the length and height coordinates in the duct, respectively;
h	is the duct height;
L	is the duct length;
u_0, u; v, Φ	are the longitudinal and transverse velocity components;
$\bar{u}$	is the average longitudinal velocity;
v_0	is the injection (suction) rate at $y = 0$;
v_1	is the injection (suction) rate at $y = h$;
ν, T	are the temperature;
p	is the pressure;
$Re = v_0 h/\gamma$;	
ρ	is the density;
ν	is the kinematic viscosity;
Nu	is the Nusselt number;
α, β, γ	are the coefficients in the pressure-drop equations;
$Pe = PrRe$;	
μ_1, μ_2	are the eigenvalues for Eqs. (1.3) and (2.7).

LITERATURE CITED

1. H. Schlichting, Boundary-Layer Theory, 6th ed., McGraw Hill, New York (1968).
2. P. P. Lugovskoi and B. P. Mironov, Inzh.-Fiz. Zh., 8, No. 4 (1967).
3. B. P. Mironov and P. P. Lugovskoi, Inzh.-Fiz. Zh., 25, No. 2 (1973).
4. N. E. Kochin, I. A. Kibel', and N. V. Roze, Theoretical Fluid Mechanics [in Russian], Vol. 2, Fizmatgiz, Moscow (1963).